Research Article

Advances in Mechanical Engineering

Advances in Mechanical Engineering
2016, Vol. 8(12) 1–8

DOI: 10.1177/1687814016683352
aime.sagepub.com
SAGE

Generation of tooth profile for Roots rotor based on virtual linkage associated with Assur group

Yingjie Cai[1], Ligang Yao[1] and Guowu Wei[2]

Abstract

This article, for the first time, presents the generation of Roots rotor tooth profiles based on an Assur-group-associated virtual linkage method. Taking the original Roots rotor as an example, structure and geometry of the Roots rotor are introduced, and based on the principle of inversion, an equivalent virtual linkage is identified for generating dedendum tooth profile of the rotor. Using linkage decomposition associated with elemental Assur groups, algorithm for computing the tooth curve is constructed leading to the explicit expression of rotor profile and the corresponding numerical simulation, verifying the validity of the proposed approach. For demonstration purpose, the virtual linkage method is then extended to the generation of tooth profiles for the variants of Roots rotors with arc-cycloidal curves and arc-involute curves. Integrated with computer-aided design, computer-aided engineering and computer-aided manufacturing software platforms, as well as the three-dimensional printing technology, this article provides an efficient and intuitive approach for Roots rotor system design, analysis and development.

Keywords

Roots rotor, Roots blower, tooth profile generation, virtual linkage, Assur group

Date received: 4 March 2016; accepted: 16 November 2016

Academic Editor: ZW Zhong

Introduction

Since the Roots brothers patented the Roots blower in 1860, this kind of rotor and its variants have been widely used as air dischargers for diesel engines, pumps and other equipments due to its capability of providing higher and greater air flow compared to a conventional pump. In order to bring greater air flow for a Roots blower, in the past one and a half centuries, different cross-sectional designs have been proposed,[1–6] analysed and developed. Ritchie and Patterson[7] investigated the geometry of involute rotors aiming for minimizing leakage. Holmes[8] and Litvin[9] established the mathematical models for the cross sections of the Roots blower rotors with involute, cycloidal and arc tooth profiles. Litvin and Feng[10] proposed computer-aided design (CAD) approach for generating the profiles. Mimmi and Pennacchi[11,12] investigated different types of positive displacement rotary pumps and blowers. Liu et al.[13] proposed a sealing index and presented a method for the design of lobe pump with high-sealing property. Furthermore, Tong and Yang[3] proposed the pumping ratio, and Yang and Tong[14] formulated the flow rate functions, leading to the design and profile synthesis of various lobe pumps.[15] Vecchiato et al.[16] developed the rotor cross section as a combination of arcs and a

[1]School of Mechanical Engineering and Automation, Fuzhou University, Fuzhou, P.R. China
[2]School of Computing, Science & Engineering, University of Salford, Salford, UK

Corresponding author:
Ligang Yao, School of Mechanical Engineering and Automation, Fuzhou University, No. 2, Xueyuan Road, University Town, Fuzhou 350116, P.R. China.
Email: ylgyao@fzu.edu.cn

conjugated epicycloidal curve. Yao et al.[17,18] investigated the geometry of Roots rotor of arc-cycloidal profile and applied the results to the cutting and milling of three-lobe helix rotors. Using the concept of variable trochoid ratio, Hsieh and Hwang[4,19,20] developed Roots rotors of high volumetric efficiency and high-sealing property. More recently, Kang and Vu[5] proposed the epicycloidal-circular-epicycloidal (CEC) rotor profile, and Hsieh[6] applied the elliptical roulette curve to the design of rotary lobe dumps.

Profiles of the cross sections of rotors play crucial role in the Roots blowers. However, according to the literature, most of the derivations for Roots rotor tooth profiles are based on gear geometry and theory which involves establishing body-attached reference systems, equation of meshing and coordinate transformation matrices. For engineers with limited knowledge in gear geometry, such derivations, as those in the treatises of Holmes[8] and Litvin,[9] seem complex to them, but generating displacement curve of a linkage through programming associate with pre-provided Assur-group subroutines appears to be easier for them. They can effectively master and apply the latter approach for Roots rotor profile generating, manufacturing and testing. Therefore, this article proposes an Assur-group-associated virtual linkage method for generating the tooth profiles of Roots rotors of various types. The virtual linkage method has been used in multi-grasp manipulation,[21] haptic manipulation[22] and parallel mechanism synthesis,[23] but no report has been found for its application in generating rotor tooth profiles.

Kempe[24] pointed out that planar curves can be generated by linkages; theoretically, the planar curves in the cross sections of tooth profiles of Roots blowers can be produced by linkages. Hence, this article, for the first time, presents the application of virtual linkage method to the generation of Roots rotor tooth profiles. The principle of inversion, as defined in Ye et al.,[25] is used in this investigation, leading to the discovery of equivalent virtual linkages, and programming algorithms associated with Assur-group subroutines are formulated and developed, verifying and demonstrating the validity of the proposed method.

Structure and geometry of a Roots rotor

Figure 1 shows the structure a Roots blower developed in this article. It consists of two rotors, that is, rotor 1 and rotor 2. The ratio of the angular velocities between the two rotors is 1; in the practical applications, this transmission ratio is secured by a pair of equal gears that are mounted on the shafts of the two rotors (see Figure 1). Commonly, the rotors have two or three lobes, and the cross-sectional profiles of the two rotors are identical as illustrated in Figure 2. The general

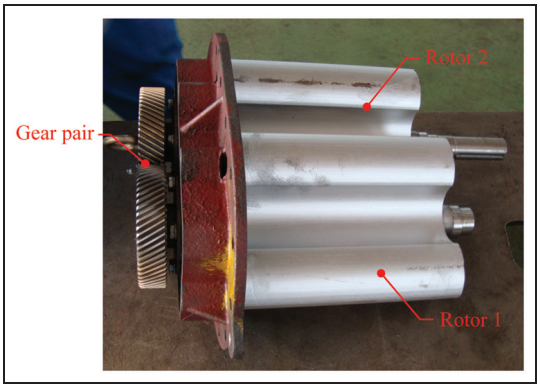

Figure 1. Structure of a Roots blower.

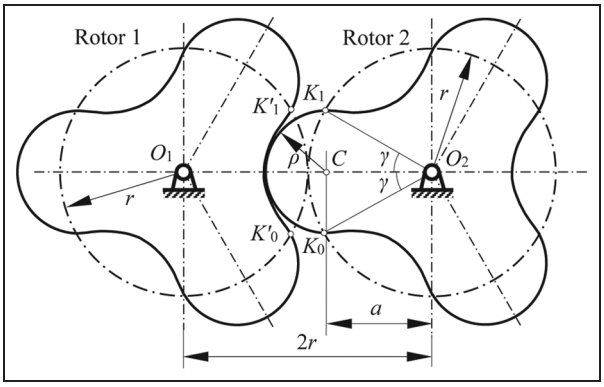

Figure 2. Geometry of rotor tooth cross-sectional profiles.

profile of a rotor tooth is formed by two types of curves, that is, the addendum profile curve, for example, curve K_0K_1 indicated in Figure 2 which is a circular arc of radius ρ centred at point C, and the dedendum profile curve, for example, curve $K'_0K'_1$ which is equidistant to the shortened epicycloid that is commonly generated through equation of meshing.[9,18,20] The addendum angle of curve K_0K_1 of a rotor with two or three lobes equals 90° and 60°, respectively, such that the value of angle γ (see Figure 2) is 45° and 30°, respectively, for two- and three-lobe rotors. In this article, we concern only rotors with three lobes, while the method presented herein be extended to rotors with two lobes.

From the above description, it can be found that the key issue to produce the full profile of a rotor lies in the creation of the dedendum curve $K'_0K'_1$. According to the literature, this curve was, in most of the cases, obtained through the traditional approach based on gear geometry, in which the generation of curve $K'_0K'_1$ involves establishing coordinate systems, transformation matrices and equation of meshing. In order to simplify the derivation and provide an efficient and intuitive way for producing the curve, based on the principle that planar curves can be generated by planar linkages,[24,26] this article proposes an alternative method based on Assur-group-associated virtual linkage.

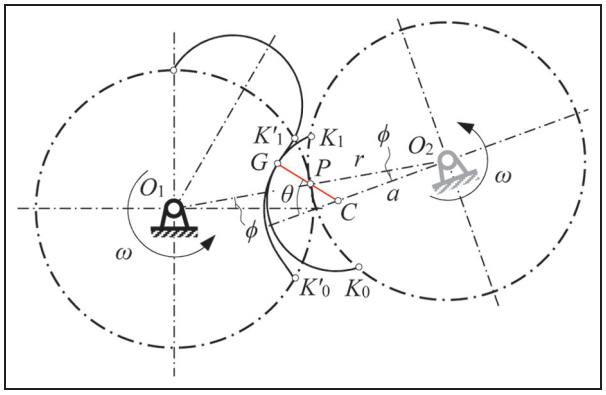

Figure 3. Principle of inversion for generation of curve $K'_0K'_1$.

Equation of meshing and identification of equivalent virtual linkage

Equation of meshing based on principle of inversion

As shown in Figure 2, when the two rotors work together, the addendum curve of rotor 2 meshes the dedendum curve of rotor 1 and vice versa. The two rotors always rotate in the opposite directions, as they are actually coordinated by a pair of gears with gear ratio 1, such that when rotor 1 rotates about O_1 by ϕ clockwise, rotor 2 will correspondingly rotate about O_2 by ϕ counter-clockwise. According to the principle of inversion,[25] this working process is equivalent to the process as indicated in Figure 3; let rotor 1 be fixed, the central point O_2 of rotor 2 rotates about O_1 by ϕ counter-clockwise and simultaneously rotor 2 rotates about O_2 by ϕ counter-clockwise. This process inversely performs the meshing between the two rotors. Thus, with the addendum curve K_0K_1 in rotor 2 being a circular arc of radius ρ centred at point C, the inverse process can lead to the generation of the dedendum curve $K'_0K'_1$ in rotor 1.

Referring to Figure 3, it can be seen that point G is the instant contact point between the two rotors at the current configuration, lying on circular arc K_0K_1, point P is the instantaneous centre of rotation and point C is the centre of arc K_0K_1. In this case, the normal at point G, which is perpendicular to the tangency of the addendum curve, that is, circular arc K_0K_1, must pass through both points P and C. Since curve K_0K_1 is a circular arc centred at C, it can be found that in any configuration during the working process, points G, P and C remain on a common straight line.

Furthermore, as indicated in Figure 3, according to the law of sine, in ΔCO_2P, it has

$$\frac{a}{\sin(\theta-\phi)} = \frac{r}{\sin(180^\circ-\theta)} \tag{1}$$

which can be simplified and rearranged in the form of function in terms of variables θ and ϕ as

$$f(\theta,\phi) = r\sin(\theta-\phi) - a\sin\theta = 0 \tag{2}$$

It can be found that equation (2) is exactly the same as the equation of meshing of the Roots rotors presented in Litvin's[9] work, which was obtained through establishing coordinate systems and the complex mathematical derivations based on gear geometry. Therefore, the above derivation of equation (2) based on the principle of inversion not only reveals an efficient and intuitive approach for establishing the equation of meshing for Roots rotor but also verifies the validity of the virtual linkage method presented in this article.

Function equivalence and the virtual linkage

Since point G is the instantaneous contact point between the two rotors, it belongs to both the addendum curve K_0K_1 in rotor 2 and the dedendum curve $K'_0K'_1$ in rotor 1. If the aforementioned inverse process continues with the rotation angle ϕ lying in the range of $[-\gamma,\gamma]$ (here, $\gamma = 30^\circ$ for the rotor with three lobes), the trajectory of point G traced on rotor 1 straightforwardly provides the dedendum curve $K'_0K'_1$.

By carefully observing and analysing the above inverse process, it can be found that point O_2 rotates about point O_1 with a constant radius of length $2r$, point C rotates about point O_2 with a constant radius of length a and line CG of length ρ rotates about point C passing through point P which is the midpoint of O_1O_2. If we virtually place revolute joints at points O_1, O_2, C and P with O_1 being a fixed pivot, a prismatic joint at point P, and replace lines O_1O_2, O_2C and CG with rigid links, a linkage can be obtained as shown in Figure 4. Since this linkage is constructed in an arbitrary configuration with point G, the trajectory of point G results in the dedendum curve $K'_0K'_1$ of rotor 1; comparing with the inverse process presented in Figure 3, we find that this linkage has the equivalent function as rotor 2 for generating tooth profile. Thus, this linkage is termed as virtual linkage which can virtually be used to generate a specified tooth profile.

Assur-group-based linkage decomposition and computation of dedendum curve

The analysis of multi-bar linkage is complex if one tries to solve the linkage as a whole system, but the problem becomes easier if the linkage is decomposed into several elementary Assur groups.[27] There are different Assur groups such as Link group, RRR group and RPR group where R stands for revolute joint and P denotes

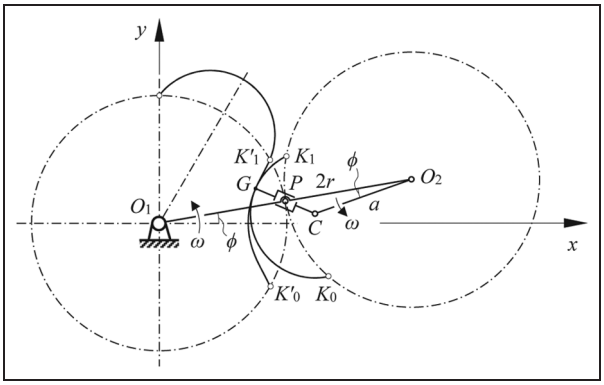

Figure 4. Equivalent virtual linkage for generating curve $K_0'K_1'$.

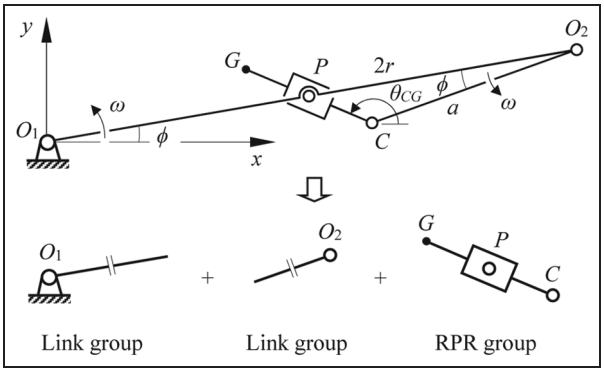

Figure 5. Decomposition of the virtual linkage and the Assur groups.

Table 1. Algorithm for computing dedendum curve $K_0'K_1'$.

1	Input: r, a and ρ, which are structure parameters
2	Open #1: name "Data_curve", Create new
3	For $\phi = 0$ to γ step $\pi/180$
4	Call **Link**(0, 0, ϕ, r, X_P, Y_P)
5	Call **Link**(0, 0, ϕ, $2r$, X_{O2}, Y_{O2})
6	Call **Link**(X_{O2}, Y_{O2}, $\pi + 2\phi$, a, X_C, Y_C)
7	Call **RPR**(0, X_C, Y_C, X_P, Y_P, 0, θ_{CG})
8	Call **Link**(X_C, Y_C, θ_{CG}, ρ, X_G, Y_G)
9	Print #1: X_G, Y_G
10	Next ϕ
11	End

prismatic joint. The formulations and their associated programming subroutines for the elemental Assur groups can be found in Ye et al.[25]

According to the Assur groups, the virtual linkage indicated in Figure 4 can be decomposed into two Link groups and one RPR group as shown in Figure 5. One Link group rotates about the fixed pivot O_1 and the other one rotates about the floating point O_2. Once the configurations of links O_1O_2 and O_2C are determined, the position of point G can be calculated from the RPR group, providing the coordinates for generating curve $K_0'K_1'$.

Based on the Assur groups in Figure 5, using the algorithm in Table 1 which is associated with the subroutines for the Assur groups provided in Ye et al.,[25] the position of point G can be obtained in terms of input angle ϕ.

For the algorithm presented in Table 1, three structure parameters r, a and ϕ are defined, and the variable is angle ϕ. The length of link O_1O_2 is $2r$ with point P being the midpoint, the length of link O_2C is a and the length of link CG is ρ. A coordinate system is established at point O_1 with the x-axis directing horizontally rightwards and the y-axis pointing vertically upwards. In Table 1, lines 4 and 5 use the **Link** subroutine to calculate the positions of points P and O_2, respectively. With the position of point O_2 obtained from line 5, line 6 leads to the position of point C. Then, substituting positions of points C and P into line 7 by calling the **RPR** subroutine, it gives the angle between link CG and the x-axis, which is denoted as θ_{CG}. With position of point C and angle θ_{CG}, line 8 uses **Link** subroutine to compute the coordinates of point G. Line 9 collects the coordinates of point G for generating curve $K_0'K_1'$.

Based on the symbolic calculation, programme according to the above algorithm explicitly results in the position of point G as

$$\begin{bmatrix} x_G \\ y_G \end{bmatrix} = \begin{bmatrix} 2c\phi & -c2\phi \\ 2s\phi & -s2\phi \end{bmatrix} \begin{bmatrix} r \\ a \end{bmatrix} + \rho \begin{bmatrix} c(\theta - 2\phi) \\ s(\theta - 2\phi) \end{bmatrix} \quad (3)$$

with the structure parameters and angles θ and ϕ satisfying $r\sin(\theta - \phi) - a\sin\theta = 0$. In equation (3), s and c, respectively, stand for the sine and cosine functions.

The results in equation (3) is, again, exactly the same as the results obtained in Litvin's derivation based on gear geometry.[9] Thus, we assume that the curves obtained through virtual linkage method is exactly the same as the ones obtained by gear geometry.

By assigning $r = 40\,\text{mm}$, $a = 32\,\text{mm}$ and $\rho = \sqrt{r^2 + a^2 - 2ra\cos 30^\circ} = 20.17\,\text{mm}$, and giving the value of angle ϕ in the range of $[-30^\circ, 30^\circ]$, a numerical example is subsequently implemented so as to demonstrate the validity of the proposed virtual linkage method. Figure 6 shows the dedendum curve $K_0'K_1'$ that is generated using the Assur-group-associated virtual linkage method. By adding the addendum curve which is a circular arc of radius ρ centred on a circle of radius a about point O_1, and evenly distributing the dedendum and addendum curves around point O_1, the completed tooth profile of a Roots rotor can be obtained as indicated in Figure 6. Furthermore, by changing the ratio a/r complying with $a/r < 0.9670$ so as to eliminate curves with singularity,[9] various tooth profiles can be achieved by the proposed virtual linkages method, as

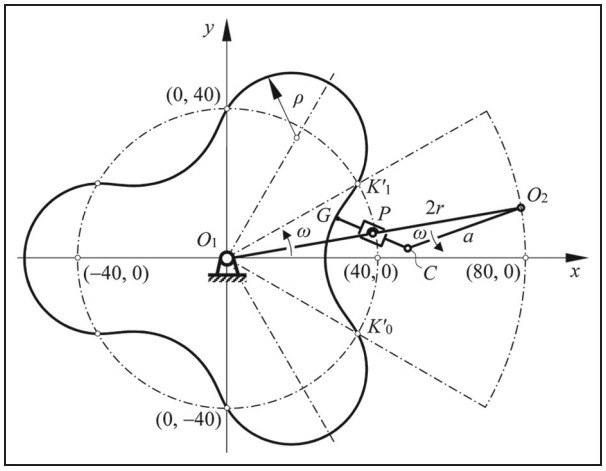

Figure 6. Generation of dedendum curve $K_0'K_1'$ with virtual linkage.

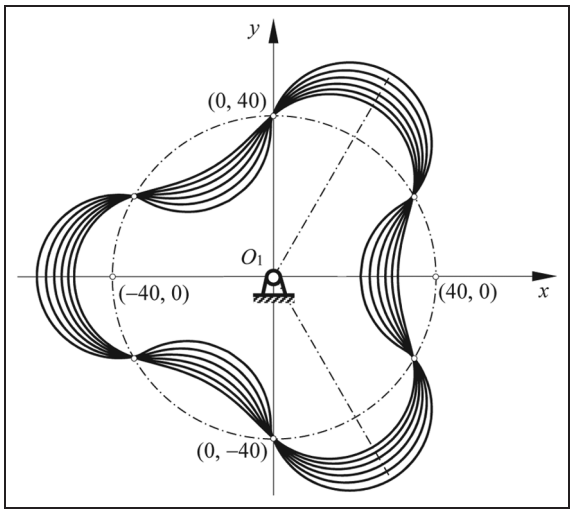

Figure 7. Rotor tooth profiles with various a/r ratios.

illustrated in Figure 7, providing alternatives for different applications. Prototype of a Roots rotor with its tooth profiles generated using the present method was fabricated and constructed in this article as shown in Figure 1.

Extended applications of the proposed virtual linkage method

The virtual linkage method proposed in this article can further be applied to the tooth profile generation for Roots blowers with arc-cycloidal and arc-involute curves.

Generation of arc-cycloidal tooth profile

Figure 8 shows the cross-sectional profiles of a pair of arc-cycloidal rotors. The profiles of the two rotors are identical. In each rotor, the dedendum tooth curve, for example, curve FG in rotor 2, is a circular arc centred at the reference circle of radius r, and the addendum tooth curve, for example, curve AD in rotor 1, is composed of three segments as cycloidal flank AB, a tip circular arc BC centred at point E lying on the reference circle of radius r and another cycloidal flank CD. The two cycloidal flanks AB and CD are symmetric with respect to the line O_1E. For a three-lobe rotor, the angle formed by the two end points of the addendum tooth curve and the centre of the rotor, for example, $\angle AO_1D$, is equal to 60°, and the angle formed by the end points of the dedendum tooth curve and the centre of the rotor, for example, $\angle FO_2G$, is equal to 60°. The radius ρ of the convex and concave circular arcs is determined by the structure parameters as $\rho = r\sqrt{2(1-\cos 30°)}$.

In this type of Roots rotor, the two circular arcs, that is, the root circular arc and tip circular arc, can be generated straightforwardly; to obtain the completed tooth profile, it relies on the finding of an efficient approach to generate the cycloidal flanks. Taking the cycloidal flank CD in Figure 8 as an example, we use the principle of inversion to investigate the curve in the meshing process. Assuming that rotor 1 is fixed, by rotating O_1O_2 about O_1 by ϕ and simultaneously rotating rotor 2 itself about O_2 by the same angular displacement ϕ as indicated in Figure 8, it can be found that during the meshing process, the cycloidal curve CD keeps on contacting with the end point G of the circular arc FG. This implies that drawing the trajectory of point G in rotor 2 on the cross-sectional plane of rotor 1 will provide the cycloidal curve CD in rotor 1. Since the lengths of O_1O_2 and O_2G are constant, the above process can be equivalently realized by a virtual $2r$ linkage as indicated in Figure 9 with O_1 being a fixed revolute joint and O_2 being a floating revolute joint connecting the two serial links O_1O_2 and O_2G.

According to Assur group, the equivalent virtual $2r$ linkage shown in Figure 9 can be decomposed into two Link groups. It should be pointed out that the virtual $2r$ linkage can generate the cycloidal flank for theoretical profile as indicated in thick solid line in Figure 9; however, in the practical cases, in order to avoid interference between the two rotors to provide smooth rotation, there is a fine clearance Δ between the theoretical profile and the practical profile (see Figure 9). Therefore, for each theoretical point G, there is a corresponding practical point G_1, in order to compute the position for point G_1, it costs effort based on gear geometry method; but through virtual linkage method, this can be achieved through the introduction of an imaginary **RRR** group consisting of three pivots P, O_2 and G. Using the subroutines for the Assur groups provided in Ye et al.,[25] algorithm as schemed in Table 2 can be constructed to generate the theoretical and practical cycloidal flanks.

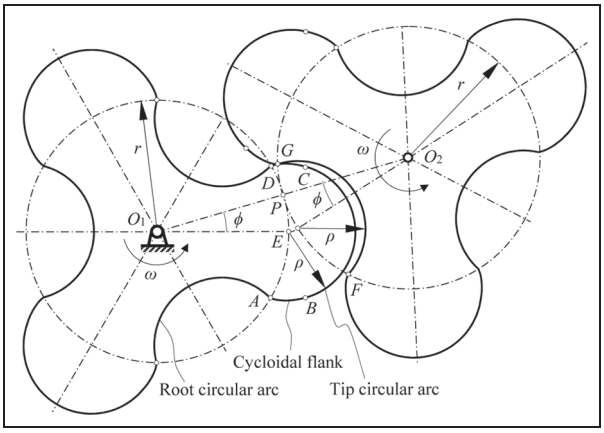

Figure 8. Geometry of an arc-cycloidal profile and cycloidal curve *DC* in meshing process.

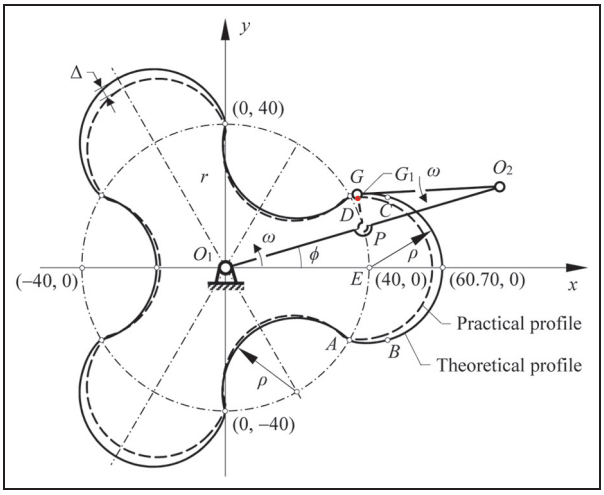

Figure 9. Generation of cycloidal curve through an equivalent virtual linkage.

In the algorithm, lines 4, 5 and 6 call the **Link** subroutine to calculate positions of points P, O_2 and G, respectively, and trajectory of point G provides the theoretical cycloidal flank CD. Line 7 calculates the length between points P and G, and line 8 uses the **RRR** subroutine to calculate the angle between line PG and the x-axis, denoted by θ_{PG}. Subsequently, with the position of point P and angle θ_{PG} being provided, line 9 generates the position for point G_1 leading to the practical cycloidal flank $C'D'$ (which is not indicated in the figure). Consequently, line 10 stores the coordinates of point G_1 for generating the practical cycloidal flank $C'D'$.

Symbolic computing of the above programme leads to the implicit expression of the cycloidal curve CD as

$$\begin{bmatrix} x_G \\ y_G \end{bmatrix} = \begin{bmatrix} \cos\phi & \cos(5\pi/6 + 2\phi) \\ \sin\phi & \sin(5\pi/6 + 2\phi) \end{bmatrix} \begin{bmatrix} 2r \\ r \end{bmatrix} \quad (4)$$

Table 2. Algorithm for computing the cycloidal flank.

1	Input: r, Δ
2	Open #1: name "Data_cycloidal", Create new
3	For $\phi = 0$ to $30\times\pi/180$ step $\pi/180$
4	Call **Link**(0, 0, ϕ, r, X_P, Y_P)
5	Call **Link**(0, 0, ϕ, $2r$, X_{O2}, Y_{O2})
6	Call **Link**(X_{O2}, Y_{O2}, $5\pi/6 + 2\phi$, r, X_G, Y_G)
7	$L_{PG} = \sqrt{(X_P - X_G)^2 + (Y_P - Y_G)^2}$
8	Call **RRR**(X_P, Y_P, X_{O2}, Y_{O2}, L_{PG}, r, θ_{PG}, θ_{O2G})
9	Call **Link**(X_P, Y_P, θ_{PG}, $L_{PG} - \Delta$, X_{G1}, Y_{G1})
10	Print #1: X_{G1}, Y_{G1}
11	Next ϕ
12	End

with angles ϕ complying with $0 \le \phi \le \pi/6$. This equation is exactly the same as the one obtained in Yao et al.[18] based on gear geometry.

Once curves CD and $C'D'$ are obtained, mirroring them with respect to the x-axis results in curves AB and $A'B'$. A numerical example of a rotor with arc-cycloidal tooth profile is then implemented using the proposed virtual linkage approach, and the results are illustrated in Figure 9. The radius of the reference circle in the example is $r = 40$ mm such that the radius of the tip and root circular arcs is $\rho = r\sqrt{2(1 - \cos 30°)} = 20.70$ mm; for illustrative purpose, the clearance Δ is given as 2.5 mm.

Rotor with arc-involute tooth profile

The virtual linkage method can further be applied to the generation of the tooth profile containing involute flank.

Due to its merit of smooth transmission and the mature manufacturing process for involute profile, involute curve is also used in Roots rotor. In such a rotor, the tooth profile contains three curves, that is, the convex tip circular arc AB of radius ρ centred at the pitch circle, the involute flank BC and the concave root circular arc CD of radius ρ centred at the pitch circle as illustrated in Figure 10. Both the tip and the root circular arcs are tangent to the involute flank. According to the property of an involute, there exits the length of KG denoted as L_{KG} which is equal to $r_b\phi$, and the generation of the involute flank of the rotor can be realized by a virtual $2r$ linkage with two revolute joints located at the fixed pivot O_1 and the floating pivot K, respectively, connecting the constant link O_1K and the variable link KG as shown in Figure 10. In this case, in order to produce curve CD, only Assur-group **Link** is requested and the algorithm for calculating the position of point G can be constructed as presented in Table 3.

From the symbolic calculation of the above programme, the position of point G can be obtained as

$$\begin{bmatrix} x_G \\ y_G \end{bmatrix} = \begin{bmatrix} 1 & \phi \\ -\phi & 1 \end{bmatrix} \begin{bmatrix} r_b\cos(\phi + \phi_0) \\ r_b\sin(\phi + \phi_0) \end{bmatrix} \quad (5)$$

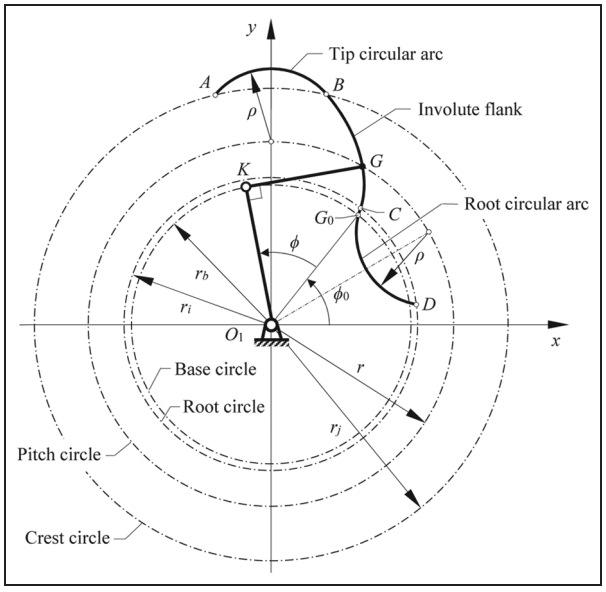

Figure 10. Geometry and tooth curves of a involute rotor.

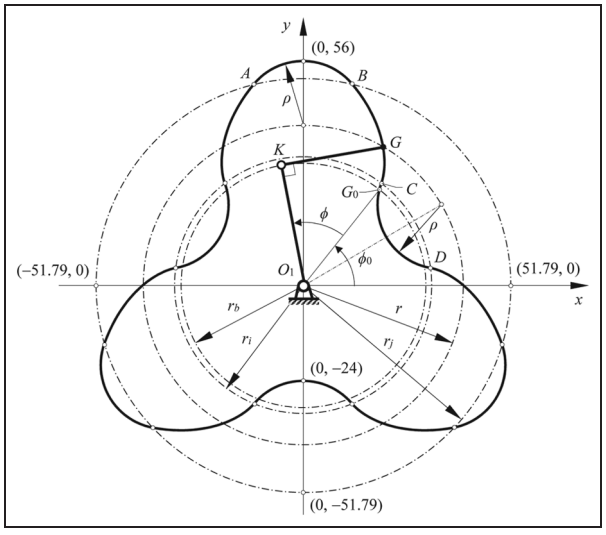

Figure 11. Tooth profile of an involute Roots rotor generated by virtual linkage.

Table 3. Algorithm for computing the involute flank.

1	Input: r_b, ϕ_0
2	Open #1: name "Data_involute", Create new
3	For $\phi = 0$ to $80\times\pi/180$ step $\pi/180$
4	Call **Link**(0, 0, ($\phi_0 + \phi$), r_b, X_K, Y_K)
5	LKG = $r_b \times \phi$
6	Call **Link**(X_K, Y_K, $\phi + \phi_0 - \pi/2$, L_{KG}, X_G, Y_G)
7	Print #1: X_G, Y_G
8	Next ϕ
9	End

which again verifies the validity of the proposed virtual linkage approach.

Then, based on the geometric constraints and relations presented in Ritchie and Patterson,[7] a numerical example is conducted leading to the completed tooth profile of a involute Roots rotor as shown in Figure 11.

Hence, the Assur-group-associated virtual linkage method presented in this article for the generation of Roots rotor tooth profiles is efficient, and from engineering point of view, it is intuitive. It provides an alternative approach for generating tooth profiles for Roots blowers. Integrating this approach with CAD, computer-aided engineering (CAE) and computer-aided manufacturing (CAM) software platforms, and the emerging three-dimensional (3D) printing technology, this method can lead to better designing, analysis and simulation for Roots rotor systems.

Conclusion

The Assur-group-associated virtual linkage method was, for the first time, applied for the generation of tooth profiles of Roots rotors. By characterizing the geometry and meshing properties of the original Roots rotors, the procedure for identifying the equivalent virtual linkage was presented; then, using linkage decomposition and its association with Assur group, algorithm for calculating the tooth profiles was constructed, leading to the explicit expression of position coordinates of the tooth profiles. Subsequently, the results were compared and verified with those obtained based on gear geometry approach. Numerical example was provided demonstrating the validity of the proposed method. Furthermore, the method was extended to the generation of tooth profiles of the variants of Roots rotors with arc-cycloidal and arc-involute curves. Hence, this article has provided a new, efficient and intuitive approach for the generation of Roots rotor tooth profiles, and considering the programme-based characteristics of the proposed method, it can be integrated with modern CAD, CAE and CAM platforms, as well as the emerging 3D printing technology, providing background for more effective Roots rotor system design and development.

Declaration of conflicting interests

The author(s) declared no potential conflicts of interest with respect to the research, authorship, and/or publication of this article.

Funding

The author(s) disclosed receipt of the following financial support for the research, authorship, and/or publication of this article: This study was supported by the National Natural Science Foundation of China (NSFC) under grant nos

51275092 and 51375013 and the VC ECR scholarship at the University of Salford under grant no. SGGK07.

References

1. Hallett GEA. *Roots blower*. US2014932A Patent, 1935.
2. Kaga M and Takeda T. *Roots type blower with reduced gaps between the rotors*. US466384 Patent, 1987.
3. Tong SH and Yang DCH. On the generation of new lobe pumps for higher pumping flowrate. *Mech Mach Theory* 2000; 35: 997–1012.
4. Hwang YW and Hsieh CF. Study on high volumetric efficiency of the roots rotor profile with variable trochoid ratio. *Proc IMechE, Part C: J Mechanical Engineering Science* 2006; 220: 1375–1384.
5. Kang YH and Vu HH. A newly developed rotor profile for lobe pumps: generation and numerical performance assessment. *J Mech Sci Technol* 2014; 28: 915–926.
6. Hsieh CF. A new curve for application to the rotor profile of rotary lobe pumps. *Mech Mach Theory* 2015; 87: 70–81.
7. Ritchie JB and Patterson J. Geometry and leakage aspects of involute rotors for roots blower. *Proc Inst Mech Eng* 1968; 183: 707–724.
8. Holmes WT. *Plane geometry of rotors in pumps and gears*. Manchester: Manchester Scientific Publishing, 1978.
9. Litvin FL. *Gear geometry and applied theory*. Upper Saddle River, NJ: Prentice Hall, 1994.
10. Litvin FL and Feng PH. Computerized design and generation of cycloidal gearings. *Mech Mach Theory* 1996; 31: 891–911.
11. Mimmi G and Pennacchi P. Involute gear pumps versus lobe pumps: a comparison. *J Mech Design* 1997; 119: 458–465.
12. Mimmi G and Pennacchi P. Analytical model of a particular type of positive displacement blower. *Proc IMechE, Part C: J Mechanical Engineering Science* 1999; 213: 517–526.
13. Liu HC, Tone SH and Yang DCH. Trapping-free rotors for high-sealing lobe pumps. *J Mech Design* 2000; 122: 536–542.
14. Yang DCH and Tong SH. The specific flowrate of deviation function based lobe pumps – derivation and analysis. *Mech Mach Theory* 2002; 37: 1025–1042.
15. Tong SH and Yang DCH. Rotor profiles synthesis for lobe pumps with given flow rate functions. *J Mech Design* 2005; 127: 287–294.
16. Vecchiato D, Demenego A, Litvin FL, et al. Geometry of a cycloidal pump. *Comput Method Appl M* 2001; 190: 2309–2330.
17. Yao L, Ye Z, Cai H, et al. Design of a milling cutter for a novel three-lobe arc-cycloidal helical rotor. *Proc IMechE, Part C: J Mechanical Engineering Science* 2004; 218: 1233–1241.
18. Yao L, Ye Z, Dai JS, et al. Geometric analysis and tooth profiling of a three-lobe helical rotor of the roots blower. *J Mater Process Tech* 2005; 170: 259–267.
19. Hsieh CF and Hwang YW. Study on the high-sealing of roots rotor with variable trochoid ratio. *J Mech Design* 2007; 129: 1278–1284.
20. Hsieh CF and Hwang YW. Tooth profile of a roots rotor with a variable trochoid ratio. *Math Comput Model* 2008; 48: 19–33.
21. Williams D and Khatib O. The virtual linkage: a model for internal forces in multi-grasp manipulation. In: *Proceedings of the IEEE international conference on robotics and automation*, Atlanta, GA, 2–6 May 1993, pp.1025–1030.
22. Nahvi A, Nelson DD., Hollerbach JM, et al. Haptic manipulation of virtual mechanisms from mechanical CAD designs. In *Proceedings of the IEEE international conference on robotics and automation*, Leuven, Belgium, 20 May 1998, pp.375–380.
23. Kong X and Gosselin C. *Type synthesis of parallel mechanisms*. Berlin: Springer, 2007.
24. Kempe AB. On a general method of describing plane curves of the nth degree by linkwork. *P Lond Math Soc* 1876; 7: 213–216.
25. Ye Z, Lan Z and Smith MR. *Mechanisms and machine theory*. Beijing, China: Higher Education Press, 2001.
26. Nolle H and Hunt KH. Optimum synthesis of planar linkages to generate coupler curves. *J Mechanisms* 1971; 6: 267–287.
27. Assur LW. *Isledovanie ploskich sterschnich mechanismow s nischnimi parami*. Petrograd: Iswestia Petrogradskowo Politechn, 1915 [1914].